Received: 17 December 2018 | Revised and accepted: 11 April 2019 | Uncorrected manuscript published: 15 April 2019

DOI: 10.1111/tra.12648

ORIGINAL ARTICLE

Traffic WILEY

Shear stress and oxygen availability drive differential changes in opossum kidney proximal tubule cell metabolism and endocytosis

Qidong Ren[1,2] | Megan L. Gliozzi[2] | Natalie L. Rittenhouse[3] | Lia R. Edmunds[4] | Youssef Rbaibi[2] | Joseph D. Locker[5] | Amanda C. Poholek[3] | Michael J. Jurczak[4] | Catherine J. Baty[2] | Ora A. Weisz[2]

[1]School of Medicine, Tsinghua University, Beijing, China

[2]Renal-Electrolyte Division, Department of Medicine, University of Pittsburgh School of Medicine, Pittsburgh, Pennsylvania

[3]Department of Pediatrics, University of Pittsburgh School of Medicine, Pittsburgh, Pennsylvania

[4]Division of Endocrinology and Metabolism, Department of Medicine, University of Pittsburgh School of Medicine, Pittsburgh, Pennsylvania

[5]Department of Pathology, University of Pittsburgh School of Medicine, Pittsburgh, Pennsylvania

Correspondence
Ora A. Weisz, Renal-Electrolyte Division, Department of Medicine, University of Pittsburgh School of Medicine, Pittsburgh, PA 15261.
Email: weisz@pitt.edu

Funding information
National Center for Advancing Translational Sciences, Grant/Award Number: TL1 TR001858; National Institute of Diabetes and Digestive and Kidney Diseases, Grant/Award Numbers: F32 DK079307, P30 DK079307; National Institutes of Health, Grant/Award Numbers: R01 DK100357, R01 DK101484, R01 DK114012, R03 DK112044, T32 DK007052, T32 DK061296; China Scholarship Council; University of Pittsburgh Center for Research Computing; Pittsburgh Center for Kidney Research, Grant/Award Number: P30 DK079307

Peer Review
The peer review history for this article is available at https://publons.com/publon/10.1111/tra.12648/

Abstract

Kidney proximal tubule (PT) cells have high-metabolic demands to drive the extraordinary ion and solute transport, water reabsorption, and endocytic uptake that occur in this nephron segment. Increases in renal blood flow alter glomerular filtration rate and lead to rapid mechanosensitive adaptations in PT transport, impacting metabolic demand. Although the PT reabsorbs essentially all of the filtered glucose, PT cells rely primarily on oxidative metabolism rather than glycolysis to meet their energy demands. We lack an understanding of how PT functions are impacted by changes in O_2 availability via cortical capillaries and mechanosensitive signaling in response to alterations in luminal flow. Previously, we found that opossum kidney (OK) cells recapitulate key features of PT cells in vivo, including enhanced endocytic uptake and ion transport, when exposed to mechanical stimulation by culture on an orbital shaker. We hypothesized that increased oxygenation resulting from orbital shaking also contributes to this more physiologic phenotype. RNA seq of OK cells maintained under static conditions or exposed to orbital shaking for up to 96 hours showed significant time- and culture-dependent changes in gene expression. Transcriptional and metabolomics data were consistent with a decrease in glycolytic flux and with an increased utilization of aerobic metabolic pathways in cells exposed to orbital shaking. Moreover, we found spatial differences in the pattern of mitogenesis vs development of ion transport and endocytic capacities in our culture system that highlight the complexity of O_2-dependent and mechanosensitive crosstalk to regulate PT cell function.

KEYWORDS
endocytosis, glycolysis, kidney, metabolomics, oxygen, shear, transcriptome

1 | INTRODUCTION

Kidney proximal tubule (PT) cells recover 65% of filtered ions, metabolites and essentially all of the glucose and protein that escapes the glomerular filtration barrier. To accomplish this, PT cells maintain unique morphologic characteristics. These include an apical brush border membrane to maximize capture of ions, metabolites, and filtered proteins from the glomerular filtrate and a highly invaginated basolateral membrane replete with the Na^+/K^+-ATPase needed to drive ion and water reabsorption. The metabolic demands of the PT are extraordinary, and require efficient delivery of O_2, which is mediated by the very high blood flow to the kidneys (~25% of cardiac output).[1] Typically, PT cells rely on oxidative metabolism fueled largely by lactate, glutamine and fatty acid β-oxidation to maintain ATP and reduced nicotinamide adenine dinucleotide (NADH) levels necessary to maintain the functions of this nephron segment.[2,3] This is in contrast to other kidney cell types that primarily depend on glucose to drive their energy needs.[2] The reliance of PT cells on other fuels may reflect the need to access more highly efficient metabolic pathways to support ATP and NADH production. Alternatively or in addition, because the PT plays an essential role in reabsorbing filtered glucose, these cells must disconnect their metabolic demands from the large variations in their cytoplasmic glucose levels that accompany feeding/fasting cycles.

Replicating *in vivo* metabolism in culture models is important for developing a comprehensive understanding of kidney disease etiology and progression. Studying PT function in cell culture has been challenging because many of the available model cell lines fail to replicate key features of this nephron segment. Moreover, primary cell cultures isolated from kidney cortex tend to rapidly dedifferentiate. We have found that culturing opossum kidney (OK) cells under orbital shear stress results in dramatic upregulation of transport and trafficking proteins, enhanced endocytic capacity, increased apical microvilli and basolateral invaginations and mitochondrial and lysosomal biogenesis.[4] Consistent with the need for increased energy production to maintain these morphological and functional changes, we also observed a significant increase in adenine nucleotide levels in cells cultured under orbital shaking. This new culture model thus provides a powerful system in which to examine general aspects of PT function, and specifically to address the complex interrelationships between metabolism and the initiation and progression of kidney disease.

Our orbital culture model results in both improved oxygenation and mechanosensitive stimuli that could contribute to cell differentiation. To better understand whether and how these factors contribute to enhanced PT differentiation, we performed RNA seq on cells maintained under static conditions or exposed to orbital shaking for up to 96 hours, and assessed the changes in transcription of enzymes involved in cell metabolism. Our data are consistent with a shift away from glycolytic metabolism characterized by changes in enzyme transcription, steady state metabolite levels and fuel utilization. Taking advantage of spatial differences in oxygen availability vs shear stress distribution in our culture model, we then determined whether and how these two parameters affect the development of specific PT functions in our model system.

2 | RESULTS

Transcriptional changes in metabolic enzymes induced by cell culture under orbital shear stress. We performed RNA seq on OK cells plated on filter supports and maintained under static conditions (0X orbital speed [OS] for 0, 48, 96 hours) or cultured on a rotating shaker at 146-rpm OS (1X OS) for 12, 48 and 96 hours (Figure 1A). Three samples, each consisting of RNA isolated and pooled from three independent experiments, were sequenced for each time point. Reads were processed, assigned, and adjusted for batch variation as described in Methods, and the final dataset is provided in Table S1. Principle component analysis (PCA) showed highly consistent changes in gene expression patterns among the three experiments (Figure 1B). Cells exposed to shear stress for as little as 12 hours had a significantly different transcription profile compared with the starting cell population (0 hour). Culture for 48 or 96 hours resulted in further divergence of transcripts between cells maintained on an orbital shaker vs under static conditions, and between both of these and the starting cell population (Figure 1B). In total, 1053 genes were identified whose expression is significantly different across comparison of any two conditions. Forty-four genes were differentially expressed (relative to 0 h) within 12 hours of exposure to orbital shear stress, whereas 300 to 400 genes were differentially expressed in other pairwise comparisons.

Pathway analysis highlighted several significant metabolic pathways altered in cells exposed to orbital shaking, and the top pathways identified using Ingenuity Pathway Analysis (IPA)[5] and other pathway analysis algorithms are listed in Table 1. Despite some differences in ranking, all programs identified multiple pathways involving changes in metabolism and responses to O_2 levels. Among the most common pathways identified were activation of the liver, retinoic, farnesoid, and pregnane X receptors (LXR, RXR, FXR and PXR) responsible for regulating lipid synthesis and transport, glucose metabolism and hypoxia-inducible factor (HIF)-regulated pathways. Up- and down-regulated genes were analyzed separately using IPA, and the results are summarized in Table S2. These changes are consistent with the increased lysosomal and mitochondrial biogenesis and adenine nucleotide levels we previously measured in cells exposed to orbital shear stress.[4]

We generated a heat map of metabolic enzymes whose expression was significantly affected in cross-comparisons of each condition (Figure 2). Data from the heat map and quantitative metabolomics studies described in Figure 3A are integrated in Figure 3B to show changes in transcripts and metabolites along the glycolytic and tricarboxylic acid cycle (TCA) pathways. Among the most striking changes was a dramatic upregulation of phosphofructokinase (*PFKL/PFKP*), the rate-limiting enzyme in glycolysis, in cells cultured at 0X OS and its concomitant downregulation in cells exposed to orbital shear stress.

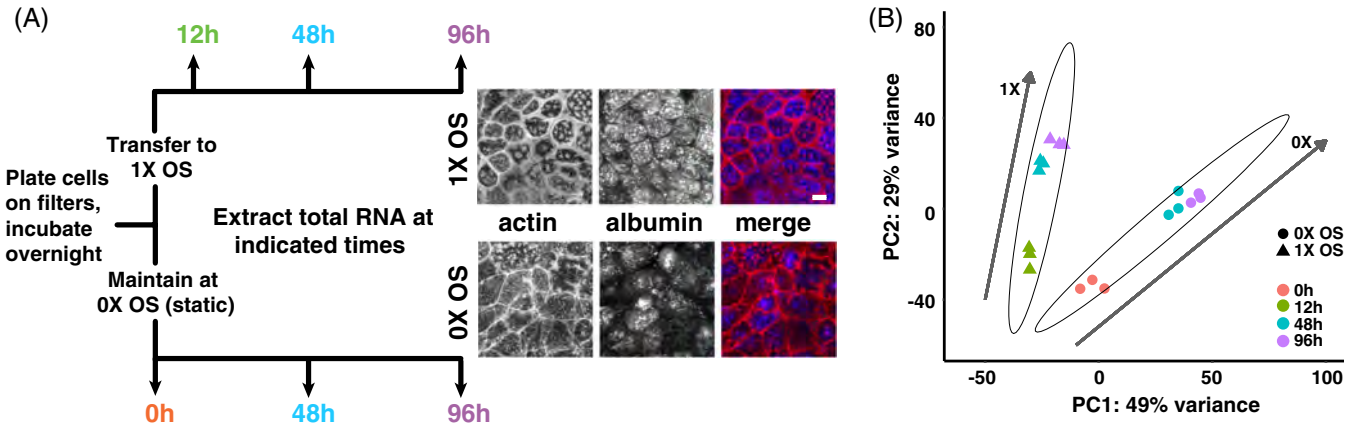

FIGURE 1 Orbital shear stress enhances OK cell differentiation and induces temporal changes in transcription. A, Flowchart of experimental design. OK cells were plated on permeable filter supports and the following day shifted to an orbital shaker at 146 rpm (1X OS) or maintained under static conditions (0X OS). One set of filters was processed immediately for isolation of RNA, and additional samples were collected at the indicated times. RNA isolated from three independent time courses was pooled for each experiment. Cells at 96 hours were exposed for 1 hour to fluorescent albumin and then fixed and stained with rhodamine-phalloidin to visualize actin in order to highlight the enhanced differentiation and endocytic capacity in cells cultured under shear stress. Scale bar: 10 μm. B, PCA of RNA seq data confirms reproducible temporal changes in transcription in three separate experiments. Each time point (0, 12, 48 and 96 hours) is denoted by a different color; data from cells cultured at 0X and 1X are shown in circles and triangles, respectively

Similarly, expression of hexokinase 1 (*HK1*) was upregulated in cells maintained for 96 hours at 0X OS. Changes in the transcription of irreversible enzymes along the glycolytic/gluconeogenic pathway (HK1, PFKL/PFKP and fructose 1,6-bis-phosphatase [FBP]) were validated using quantitative polymerase chain reaction (qPCR), although qPCR and RNA seq data for the reversible enzyme glucose 6-phosphate isomerase, whose activity is regulated by substrate availability, were discoordinate (Figure S1). Trehalase, a kidney brush border enzyme that cleaves the disaccharide trehalose into two molecules of glucose and is believed to contribute to glucose uptake by the PT,[6] was also significantly upregulated under these conditions, suggesting that cells plated on filter supports and maintained under static conditions rely increasingly on glycolysis.

By contrast, our findings are consistent with a decreased reliance on glucose as a metabolic fuel when filter-grown cells are cultured at 1X OS (Figures 2 and 3B). These cells expressed lower levels of transcripts encoding numerous glycolytic enzymes, including *HK1*, *PFKL* and the enolase isoenzymes *ENO1* and *ENO2*. We also noted changes

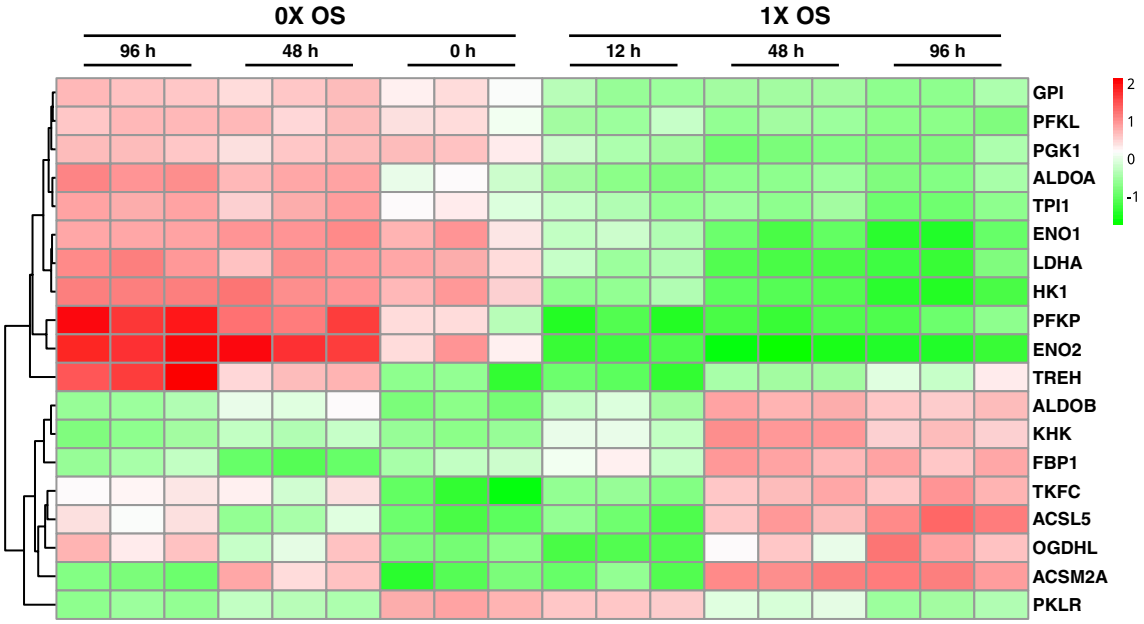

FIGURE 2 Culture under orbital shear stress alters expression of metabolic enzymes. Statistically significant ($P < 0.05$) changes in expression of metabolic enzymes identified by cross-comparisons of all conditions. Each column represents data from one experiment at a single time point. Data for each enzyme were normalized to the average counts across all 18 samples, and the fold change relative to the mean is plotted as a heat map

TABLE 1 Top 10 pathways enriched for differentially expressed genes in cells cultured at 0X vs 1X OS

IPA	BaseSpace correlation engine canonical	BaseSpace correlation engine GO
FXR/RXR activation	HIF-1-alpha transcription factor network	Response to hypoxia
LPS/IL-1-mediated inhibition of RXR function	Genes involved in biological oxidations	Response to decreased oxygen levels
LXR/RXR activation	Genes involved in metabolism of amino acids and derivatives	Extracellular matrix
Glycolysis I	Genes involved in transmembrane transport of small molecules	Xenobiotic metabolic process
PXR/RXR activation	Complement and coagulation cascades	Response to xenobiotic stimulus
Coagulation system	Extrinsic prothrombin activation pathway	Proteinaceous extracellular matrix
Acute phase response signaling	Glycolysis/gluconeogenesis	Cofactor binding
Extrinsic prothrombin activation pathway	Genes involved in glycolysis	Organic acid catabolic process
Xenobiotic metabolism signaling	HIF-2-alpha transcription factor network	Positive regulation of cell differentiation
HIF1α signaling	Genes involved in metabolism of lipids and lipoproteins	Response to metal ion

FXR, farnesoid X receptors; GO, gene ontology; IL-1, interleukin-1; LPS, lipopolysaccharide; LXR, liver X receptors; PXR, pregnane X receptors; RXR, retinoic X receptors.

in the expression of lactate dehydrogenase (LDH) A and B isoenzymes that likely impact OK cell metabolism. *LDHA* (aka the M subunit) is the predominant form expressed in liver and muscle and is kinetically adapted to convert pyruvate into lactate to promote glycolysis.[7] Conversely, *LDHB* (aka the H subunit) predominates in cardiac muscle and is optimized to convert lactate into pyruvate for entry into the TCA cycle. We observed a >4-fold reduction in *LDHA* in cells cultured at 1X OS relative to cells maintained at 0X OS. By contrast, there was a ~1.8-fold increase in *LDHB* transcripts in 1X OS cells, although this did not reach statistical significance (data included in Table S1). Indeed, the ratio of *LDHB*:*LDHA* transcripts in 1X OS cells is very similar to that reported in the S1 segment of the rat PT (5.8:1 vs 7.5:1, respectively).[8] Consistent with a reduction in LDHA enzyme expression, the rate of LDH-mediated conversion of pyruvate to lactate in lysates from cells cultured at 1X OS was roughly half that of cells cultured at 0X OS (0.41 vs 0.94 nmol/min/μL, respectively). Cells cultured at 1X OS also expressed significantly more transcripts for enzymes required for metabolism of medium and long-chain fatty acids (*ACSM2A* and *ACSL5*, respectively).

Culture-dependent changes in cell metabolites and fuel utilization. We used mass spectrometry to quantitatively compare steady-state metabolite levels in cells exposed to shear stress or maintained under static conditions for 96 hours. Raw data are shown in Figure S2, and the ratio of individual metabolites in cells cultured at 1X vs 0X OS is plotted in Figure 3A. Consistent with a reduction in glycolytic flux suggested by the decreased expression of *HK1* and *PFKL* transcripts, cells cultured at 1X OS had significantly reduced levels of glucose-6-phosphate and fructose 1,6-bisphosphate compared with cells maintained at 0X OS. OK cells cultured at 1X OS also had dramatically reduced levels of lactate and pyruvate compared with cells maintained under static conditions, consistent with rapid utilization of these metabolites at steady state. Pyruvate (via an acetyl-CoA intermediate) is converted to citrate upon entry into the TCA cycle (Figure 3B), and we found significantly increased levels of citrate and cis-aconitate in cells cultured at 1X OS. Citrate can also be produced from fatty acids via acetyl-CoA, and this could contribute as well to the difference we observed.

Finally, cells at 1X OS had significantly lower levels of glutamate and arginine compared with cells maintained at 0X OS. Glutamate is synthesized from α-ketoglutarate by glutamate dehydrogenase, a branch-point enzyme between carbon and nitrogen metabolism. In turn, glutamate can be directed either toward purine synthesis or converted to arginine. The dramatic reduction in cellular arginine levels may thus reflect the high demand for purine synthesis in cells cultured at 1X OS.

The intrinsic fluorescence of NADH and NADPH [together referred to as NAD(P)H] provides a useful tool to monitor the metabolic activity of cells.[9] We monitored changes in NAD(P)H autofluorescence to qualitatively evaluate the ability of OK cells cultured at 0X vs 1X OS to generate NAD(P)H from glucose or lactate. OK cells were cultured at 0X or 1X OS in serum-free medium (to deplete fatty acids) and then imaged in base medium spiked with glucose or lactate as described in Methods. Consistent with our previous mass spectrometry measurements, baseline NAD(P)H levels in cells incubated without these fuels were higher in cell cultured at 1X OS compared with cells maintained under static conditions (not shown).[4] Cells cultured at either 0X OS or 1 X OS were able to generate NAD(P)H when transferred to base medium containing either lactate or glucose, as seen by the increase in autofluorescence over time (Figure 4). In both cases, lactate generated more NAD(P)H than glucose. This was especially evident in cells cultured at 1X OS, where NAD(P)H levels increased dramatically within the first time point we could measure (5 minutes) and continued to rise. Glucose also elicited an obvious change in NAD(P)H levels, but more slowly. Taken together, our transcriptomic analysis and metabolomics data suggest that culturing OK cells under orbital shear stress suppresses glucose utilization and glycolysis, while increasing alternative sources of acetyl-CoA production (eg, from lactate or fatty acid oxidation), similar to the metabolism and energy utilization of the PT in vivo. However,

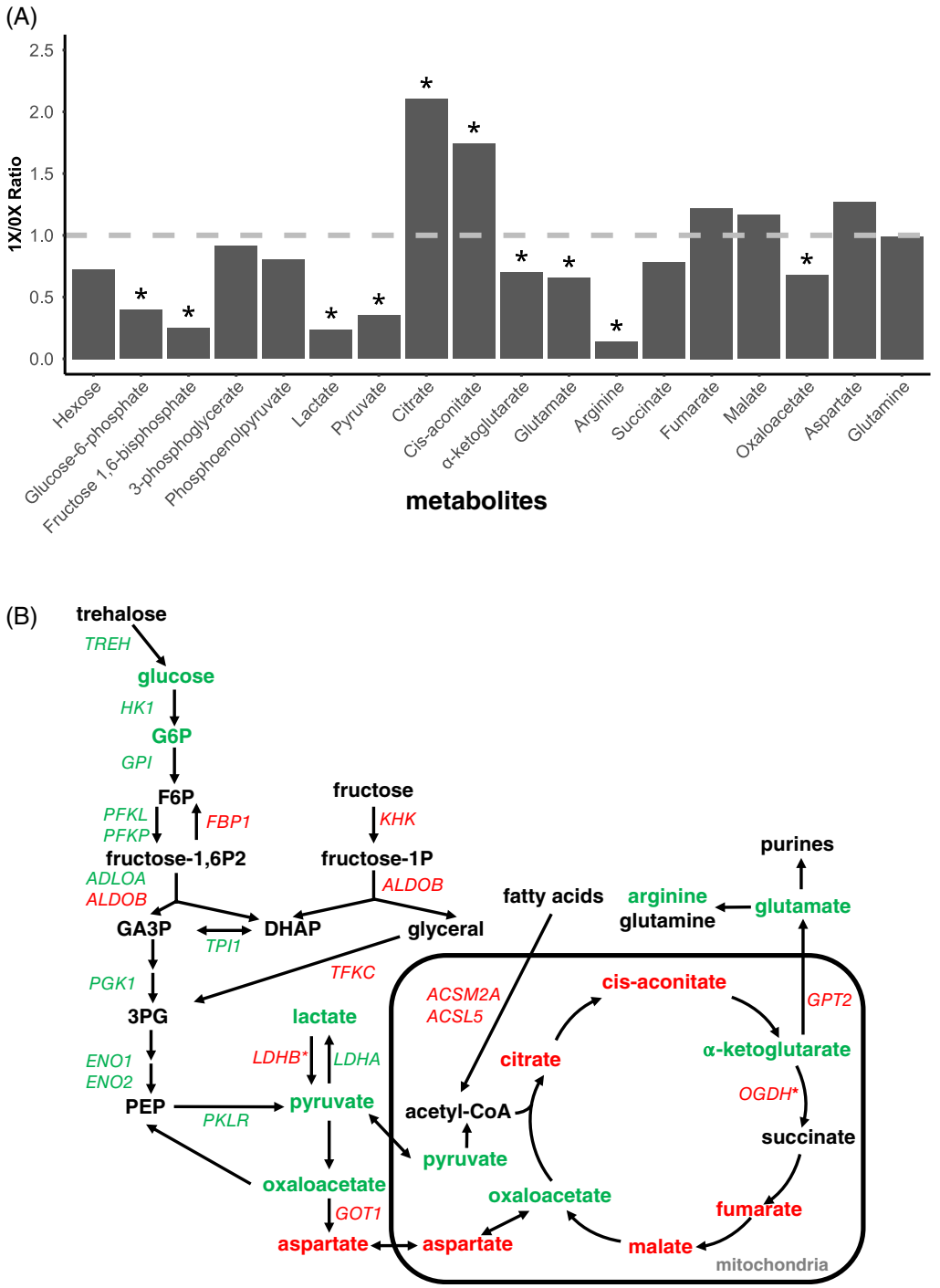

FIGURE 3 Culture under orbital shear stress alters steady-state metabolite levels in OK cells. A, Cellular metabolite levels were quantified by mass spectrometry from cells cultured at 0X or 1X OS. The fold change for each metabolite (1X/0X OS) is plotted (n = 6; **P* < 0.05 based on comparison of raw values by *t* test). B, Schematic of glycolytic and TCA pathways highlighting statistically significant changes in metabolic enzyme transcripts and metabolites measured by RNA seq and mass spectrometry, respectively. Red indicates upregulation and green indicates downregulation of genes and metabolites in cells cultured for 96 hours at 1X vs 0X OS. Asterisks denote transcripts of relevant genes that were up- or downregulated (LDHB and OGDH) but did not reach the threshold for significance in our RNA seq analysis. 3PG, 3-phosphoglycerate; DHAP, dihydroxyacetone phosphate; F6P, fructose 6-phosphate; GA3P, glyceraldehyde 3-phosphate; glycerald, glyceraldehyde; G6P, glucose 6-phosphate; OGDH, oxoglutarate dehydrogenase

fuel availability is apparently not a limiting factor for the development or maintenance of apical endocytic capacity, as neither culturing cells with supplemental lactate for 4 days nor adding it acutely (1 hour before the experiment) affected albumin uptake (not shown).

Aerobic vs mechanosensitive responses to chronic orbital shaking. Several previous studies have demonstrated a shift in metabolism toward gluconeogenesis when primary and immortalized PT cells are cultured on rocking platforms or in roller bottles.[10-18] Oxygen

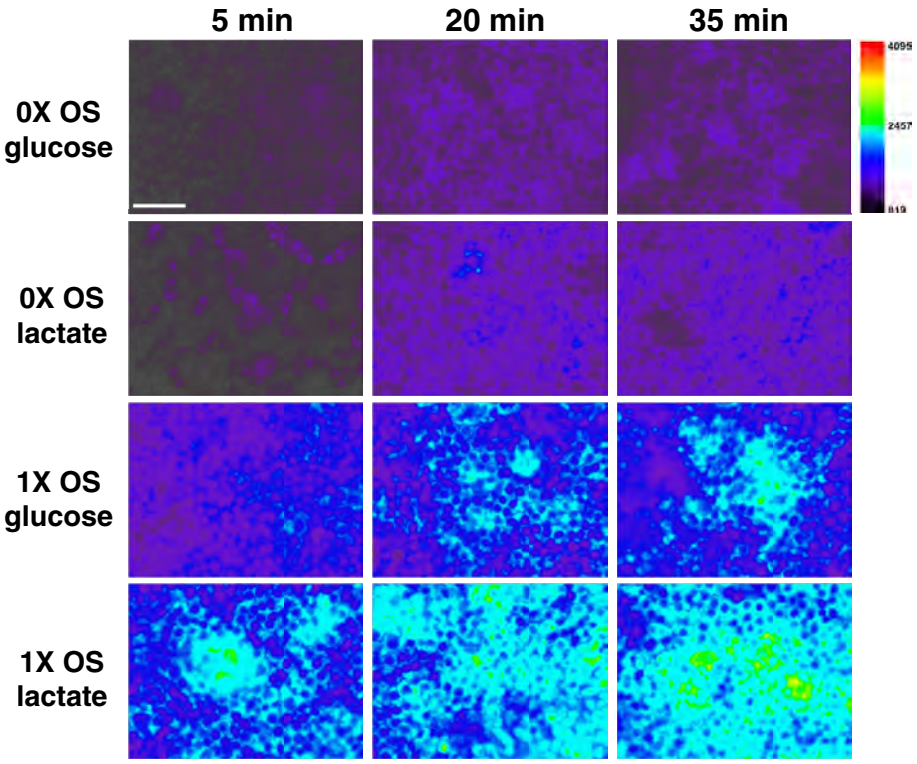

FIGURE 4 Cells cultured under orbital shear stress have higher levels of NAD(P)H and preferentially utilize lactate over glucose as fuel. Cells cultured on filter supports at 0X OS vs 1X OS were incubated in serum-free medium overnight. A strip was cut from each filter, placed on a MatTek dish, covered with base medium spiked with lactate or glucose, and overlaid with a coverslip. 4',6-diamidino-2-phenylindole (DAPI) filter NAD(P)H autofluorescence was imaged by epifluorescence microscopy. Images were collected under identical conditions every 15 minutes, and signal intensity was pseudocolored. Scale bar: 50 μm

diffusion in unstirred medium is limited, and renal epithelial cells are presumed to be hypoxic under standard culture conditions.[10,18-20] Because gluconeogenesis does not occur under anaerobic conditions, these studies concluded that improved oxygenation is the primary cause of metabolic changes. On the other hand, PT and other cells are responsive to mechanical signals that also alter transcriptional responses.[21,22] We previously found that cell culture in sealed laminar flow chambers, where oxygenation is uncoupled from shear stress, enhances endocytic capacity of OK cells, suggesting that flow sensing contributes to PT cell differentiation independent of O_2 availability.[4] However, the relationship between oxygenation, shear stress, and metabolism is complex, as many of the key mediators of metabolic regulation (eg, mammalian target of rapamycin [mTOR] and HIF1α) reciprocally regulate one another and are known to be impacted by changes in O_2 availability and shear stress.[23-25]

To assess whether enhanced oxygenation contributes to the dramatic changes in metabolism and endocytic capacity on PT function in our culture model, we asked how altering apical medium volume (ie, height, while maintaining identical nutrient availability in the basolateral medium) would affect endocytosis in cells cultured under static conditions or exposed to orbital shear stress (Figure 5). Under our standard conditions, cells are cultured with 500-μL medium added to the apical chamber and 1.5 mL added basolaterally, with daily changes to both compartments. To test the effect of medium height on endocytosis, we cultured cells at 0X or 1X OS in 100- to 800-μL apical medium, and then quantified endocytic uptake in all samples after a 15-minute incubation with AlexaFluor-647 albumin. Culture in reduced apical medium volumes has previously been demonstrated to enhance oxidative metabolism.[10] Moreover, we hypothesized that O_2

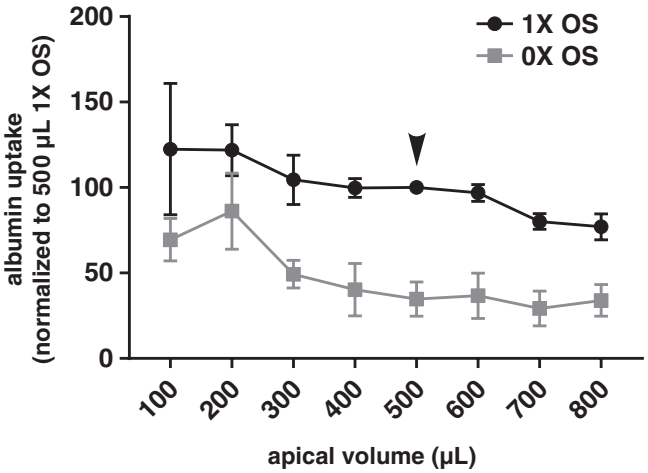

FIGURE 5 Effect of apical medium volume on endocytic uptake. OK cells plated on filters were cultured for 72 hours in 1.5-mL basolateral medium and 100- to 800-μL apical medium with daily changes. After rinsing in serum-free medium, duplicate sets of filters were incubated with 100 μL apically added AlexaFluor-647 albumin (50 μg/mL) for 15 minutes. Albumin uptake was quantified spectrophotometrically and normalized for cell number. Data for endocytic uptake by 1X OS cells cultured under our standard conditions (500-μL apical medium, arrowhead) were set to 100% in each experiment. The mean ± SD of four independent experiments is plotted. Uptake of albumin at 1X OS was significantly different (using 2-way analysis of variance with multiple comparisons [Tukey method]) from that at 0X OS at all medium volumes except 200 μL. Albumin uptake in 1X OS cells was not significantly different from the standard condition at any volume; uptake at 0X OS in 100 and 200 μL was significantly different from the standard condition; $P < 0.001$

availability would be greater and also less sensitive to differences in volume in medium subjected to continuous orbital shaking at 1X OS. Indeed, this is what we observed. Similar to our previously published findings,[4] endocytic capacity was roughly 3-fold higher in cells cultured in 500-μL apical medium at 1X OS compared with 0X OS (Figure 5, arrowhead). Endocytic uptake in cells cultured at 0X OS increased as the medium level was reduced from the standard 500 to 100 μL, with maximal endocytosis observed at 200 μL. However, albumin endocytosis in these static-grown cells, even at very low apical medium volumes, did not approach that of cells cultured at 1X OS. We conclude that changes in O_2 availability contribute in part to modulating endocytic capacity in OK cells. By contrast, decreasing apical medium volume to 200 μL in cells cultured at 1X OS had no significant effect on endocytic uptake. The opposite trend was observed when apical medium volume was increased above the usual 500 μL. Whereas there was no decrease in endocytic uptake in cells maintained at 0X OS, some reduction was evident when cells at 1X OS were cultured in ≥700 μL apical medium, presumably because these higher volumes impact cellular O_2 availability and/or shear stress (Figure 5).

The discoordinate spatial variation in oxygenation vs shear stress in our orbital culture model provides another means to distinguish between the effects of these two parameters on the development of PT cell functions. In a circular format, shear stress induced by rotation will be essentially zero at the center of each filter, and increase with the radius as fluid moves faster across the cells.[26,27] Toward the periphery of the filter, fluid shear stress is predicted to decrease as a result of frictional edge effects. By contrast, O_2 availability should be similar across the filter because of the rapid and continuous circulation of the medium. We previously demonstrated using quantitative imaging that cell culture at half of our normal OS (73 rpm, 0.5X OS) results in intermediate effects on endocytosis and proliferation between those observed in cells cultured at 0X and 1X OS.[4] Interestingly, at this suboptimal speed, there is a spatially dependent distribution of albumin uptake across the filter radius, such that endocytosis of albumin/cell increases with distance away from the center. By contrast, endocytic uptake in cells cultured at 1X OS was high and relatively uniform across the entire filter.[4] These data suggested that exposure to shear stress is important for expanding endocytic capacity in our cells.

To extend these studies, we examined how culture under shear stress impacts the spatial profiles of mitochondrial biogenesis (Cox4 expression) and ion transport (Na^+/K^+-ATPase α subunit expression) in addition to endocytic capacity (albumin uptake). For this purpose, we transitioned to culturing cells on 24-mm diameter (6-well) filters in order to provide sufficient material for spectrofluorimetric quantitation of albumin uptake and western blotting of cell lysates from the same filters. Control experiments confirmed that, similar to our results on 12-well filters, endocytic uptake in cells cultured at 0.5X OS on these larger filters was also intermediate between 0X and 1X OS (not shown). After exposing cells to fluorescent albumin for 15 minutes, a 10-mm-wide strip was cut across the length of each filter, divided into edge, middle, and center sections as shown in the diagram in Figure 6A, and the cells were solubilized. Albumin uptake was quantified using a spectrophotometer and normalized for protein recovery. Equal protein loads were western blotted to quantify Na^+/K^+-ATPase α subunit and Cox4.

As shown in Figure 6B, endocytic uptake of albumin was significantly lower in the center of the filters cultured at 0.5X OS, similar to our previous observations using quantitative imaging.[4] This was in contrast to albumin uptake in cells maintained under static conditions, which was uniform across the filter diameter. The distribution of Na^+/K^+-ATPase α subunit, measured by western blotting, paralleled that of albumin (Figure 6C). Strikingly, however, Cox4 expression distribution was uniform across the filter under both static conditions and in cells cultured at 0.5X OS (Figure 6D). Additionally (and different from albumin uptake and Na^+/K^+-ATPase α subunit expression), Cox4 levels were not increased in cells cultured at 0.5X vs 0X OS. The concordance in spatial distribution of albumin uptake and Na^+/K^+-ATPase expression with the predicted variation in shear stress across the filter diameter suggests that development of elevated endocytic and ion transport capacity in cells cultured under orbital shaking reflects (at least in part) cellular responses to shear stress. By contrast, Cox4 expression appears unaffected by shear stress at this suboptimal rotation speed.

3 | DISCUSSION

Here, we have demonstrated that OK cells exposed to continuous orbital shaking acquire metabolic characteristics more similar to those of the PT *in vivo* compared with cells maintained under static conditions. This adaptation is the result of transcriptional changes initiated within 12 hours of culture on an orbital shaker. Changes in metabolic enzyme mRNA levels are paralleled by changes in expression of ion transporters and receptors that define key PT functions, including sodium reabsorption and endocytic uptake of filtered proteins.[4] Moreover, our data suggest that improved O_2 availability resulting from enhanced medium aeration and mechanosensitive cues triggered by shear stress both contribute to the enhanced differentiated phenotype of these cells.

We found significant alterations in metabolic enzyme expression in cells cultured with orbital shaking for up to 96 hours compared with cells maintained under static conditions. The changes we observed in transcription are consistent with a switch away from glycolytic metabolism and closer to that of PT cells *in vivo*. We confirmed that cells cultured at 0X vs 1X OS accumulate different steady state metabolites consistent with the observed changes in metabolic enzyme expression. Moreover, cells cultured under orbital shear stress preferentially utilize lactate to generate NADH, similar to what has been observed in isolated perfused tubules and *in vivo*.[2] The shift from anaerobic pathways to more efficient aerobic metabolism is consistent with our previous study demonstrating a large increase in adenine nucleotide levels, including ATP and NADH, in cells cultured at 1X OS compared with 0X OS.[4] Moreover, many enzymes in the glycolytic pathway are known to have other effects on cell homeostasis independent of their

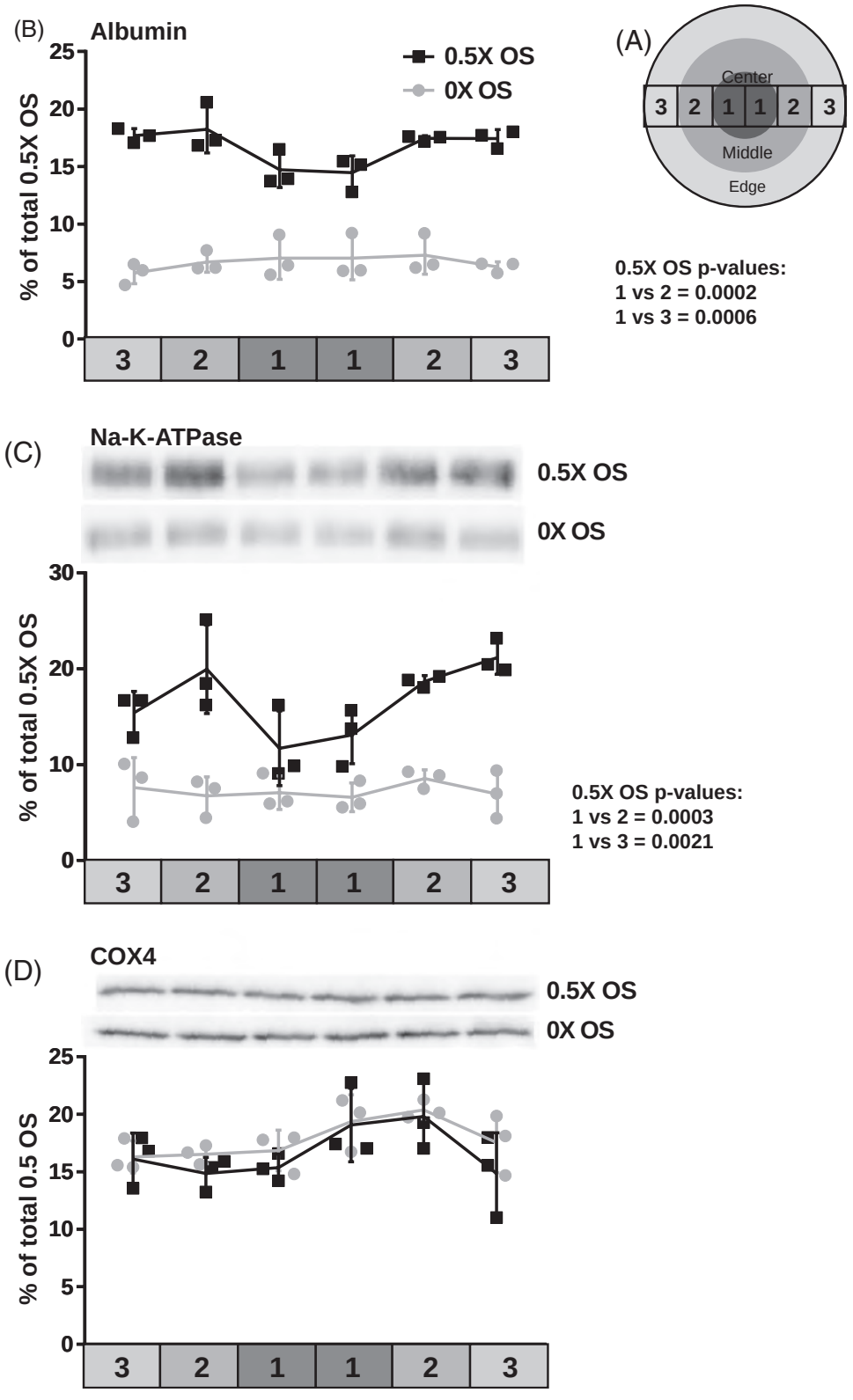

FIGURE 6 Orbital shaking differentially affects the spatial distribution of albumin uptake, Na^+/K^+-ATPase, and Cox4 expression. OK cells were cultured on 6-well filter supports under static conditions (0X OS) or at 73 rpm (0.5X OS) for 72 hours, then exposed to 50 μg/mL AlexaFluor-647 for 15 minutes. A ~24 × 10-mm strip running across the diameter of each filter was cut with a razor blade and further divided into six fractions (two each representing the edge (3), middle (2), and center (1) of the filter diameter) as shown in panel (A). Cells in each were solubilized and protein concentration was determined. Albumin uptake (B) was quantified in each fraction and normalized for protein content, and equal amounts of protein were western blotted to quantify Na^+/K^+-ATPase α subunit (C) and Cox4 levels (D). The total signal in the six sections from each 0.5X OS filter was summed, and the percentage of total in each fraction was plotted to assess distribution across the filter diameter. Individual determinations from three independent experiments are plotted, and the mean values are connected by the lines (0X OS, gray lines, 0.5X OS, black lines); Statistical significant comparisons are noted in each panel, and were calculated using combined center vs middle (1 vs 2) and edge (1 vs 3) values using 2-way analysis of variance with multiple comparisons (Tukey method)

metabolic functions, including transcriptional regulation, cytoskeletal modulation and cell motility, and cell division and survival.[28,29]

Previous studies have shown that culturing PT cells on a rocking platform alters their metabolism; a function that was attributed to enhanced oxygenation of the medium.[10,16,17] Our data suggest that increasing O_2 availability also leads to expanded endocytic capacity, as culturing cells maintained under static conditions in smaller apical medium volumes increased albumin uptake by roughly 2-fold. However, maximal uptake in these static-grown cells was still only ~70% of that measured in cells cultured at 1X OS over a wide range of apical fluid volumes, consistent with the idea that the shear stress, in addition to improved aeration, contributes to cell differentiation under our optimal culture conditions.

Both microvilli and primary cilia have been implicated in mechanosensitive responses to acute changes in shear stress in PT and other kidney cells.[30-36] Although we could not distinguish between a role for microvilli and/or primary cilia as flow sensors, our data support for a role for mechanotransduction in PT cell differentiation in response to continuous orbital shear stress. Moreover, examination of the spatial distribution of cell responses suggests that O_2 availability and shear stress contribute discoordinately to the development of PT functional characteristics in OK cells exposed to orbital shaking. We previously showed (and confirmed in our studies here) that endocytic capacity/cell varies across the diameter of filters cultured at suboptimal OS, with the least uptake near the center of the filter where shear stress is predicted to be the lowest.[4] Similarly, expression of Na^+/K^+-ATPase followed a similar pattern. By contrast, expression levels of the mitochondrial protein Cox4 were unchanged by orbital shaking and were uniformly distributed across the filter. The differential effects on Na^+/K^+-ATPase expression and endocytosis vs Cox4 expression observed under these suboptimal culture conditions suggest that shear stress and O_2 target different signaling pathways to initiate cell differentiation.

PT metabolism plays an essential role in the maintenance of kidney function, and both O_2 consumption and mechanosensitive responses to tubular flow have been implicated in disease progression.[37-39] For example, changes in energy production are a hallmark of autosomal dominant polycystic kidney disease cells. The polycystin (PC) proteins mutated in this condition are localized in part to primary cilia on distal tubule cells and have been suggested to regulate flow-dependent signaling. PCs are known to regulate Ca^{2+} signaling to mitochondria as well as mTOR complex 1 (mTORC1) signaling that could contribute to metabolic changes.[40,41] In turn, PC trafficking and activity are dependent on O_2 levels.[41] In the case of diabetes, changes in the availability of metabolic fuels alter PT metabolic pathways, leading to increased O_2 consumption that drives hypoxic injury and disease progression.[3,42]

Given the intimate connection between renal blood flow and glomerular filtration rate, it is no surprise that there is considerable crosstalk between O_2 provided by cortical capillaries and mechanosensitive responses to tubular flow. Presumably, these inputs act synergistically to link PT metabolism with ion transport and endocytosis needs. Renal O_2 levels regulate metabolic function via HIF1α, and also through mTOR.[43,44] Flow sensing mediated by primary cilia in the PT has also been demonstrated to modulate mTOR, which in turn regulates HIF-1α.[24,45] Increased flow also leads to mTOR-dependent changes in amino acid transport and endocytosis of filtered proteins that further support PT cell metabolism.[46,47] The cell culture model described here provides a useful system in which the contributions of O_2 and flow sensing to PT metabolism and other cell functions in normal and disease states can be investigated.

4 | MATERIALS AND METHODS

Cell culture and RNA seq. OK cells (RRID:CVCL_0472) were cultured as previously described.[4,48] Unless otherwise indicated, 4×10^5 cells were plated on 12-mm Transwells with 0.4-μm pore polycarbonate membrane inserts (Corning) in a 12-well plate, with 0.5-mL apical medium and 1.5-mL basolateral medium [DMEM/F12 medium (Sigma D6421) with 10% FBS (Atlanta Biologicals) and 5-mM GlutaMAX (Gibco)]. The following day (t = 0 hour), cells were transferred to an orbital platform shaker rotating at 146 rpm 1X OS or maintained under static conditions (0X OS) for 96 hours prior to use. For RNA seq studies, cells were collected using Accutase (BD Biosciences) and RNA was extracted using the Ambion PureLink RNA mini kit (ThermoFisher) at 12, 48 and 96 hours after transferring cells to 1X OS and at 0, 48 and 96 hours from cells maintained at 0X OS. RNA from three experiments was combined to create each sample, and three independent samples were sequenced for each time point. Library preparation was performed using the TruSEQ-Stranded Total RNA Sample Preparation Kit (Illumina) according to manufacturer's instructions. Following removal of ribosomal RNA, the remaining RNA was fragmented for 8 minutes, followed by reverse transcription performed. Double-stranded cDNA was subjected to 3′ adenylation and ligation of sequencing adapters. Sequencing was carried out on a NextSeq 500 (Illumina) to generate 75-bp paired-end reads. An average of 80 million paired reads was analyzed per sample.

Raw sequence reads were cleaned for adapter sequences using cutadapt[49] with default parameters. The trimmed reads were mapped to the *Monodelphis domestica* reference genome (MonDom5) using TopHat2,[50] allowing for a base-pair mismatch value of 6. Prior to calculating raw count values with the Subread package featureCounts,[51] reads aligned to mitochondrial genes and ribosomal RNA were removed.

Differential gene expression analysis was performed with the DESeq2 package,[52] using the raw count values generated from the previous step, and the batch effect was removed by adding the surrogate variable estimated by the sva package.[53] Differentially expressed genes were determined from seven different comparisons (1X96h_vs_0X0h, 1X48h_vs_0X0h, 1X12h_vs_0X0h, 0X96h_vs_0X0h, 0X48h_vs_0X0h, 1X96h_vs_0X96h, 1X48h_vs_0X48h), respectively, with parameters of alpha = 0.05 and lfcThreshold = 1. Ensembl gene IDs were converted to gene symbols to generate the list of differentially expressed metabolic genes provided in Table S1.

PCA was performed on rlog-processed raw counts using the DESeq2 package using the "plotPCA" function with default parameters except that all genes (~23 000) were used instead of the top 500.

A heatmap to identify changes in metabolic gene transcription was constructed using the seven paired comparisons. Approximately, 20 genes that encode enzymes involved in glucose, lipid, and amino acid metabolism were differentially expressed using our criteria. A dataframe was created with rlog-processed raw counts from the 18 sequenced samples. Batch effect was estimated and removed using the "sva" R package function "ComBat,"[54] and values (centered on mean expression) were plotted using Pheatmap package. (The hierarchy cluster tree distance was calculated by Euclidean method and ordered by dendsort package.[55])

Pathway analysis was performed using IPA, DAVID, Panther Pathway, BaseSpace Correlation Engine, and MetaCore. Results generated

from software packages except DAVID and Panther Pathway were based on human, mouse and rat databases and cross-compared with one another to increase the reliability.

Metabolomic analysis by untargeted high-resolution liquid chromatography-mass spectrometry. Metabolic quenching was performed by mechanical homogenization of filter-grown OK cells cultured for 96 hours at 0X or 1X OS in liquid nitrogen. The polar metabolite pool was extracted using ice-cold 80% methanol in water with 0.1% formic acid at a ratio of 15 μL per mg of dry tissue. Deuterated (D4)-taurine (100 μM; Sigma) was added to 300 μL of sample as an internal standard. The supernatant was cleared of protein by centrifugation at 16000x*g*, dried under nitrogen gas and resuspended in 40-μL 1.5-mM ammonium fluoride in water. Five microliters of reconstituted sample was subjected to online liquid chromatography–mass spectrometry (LC-MS) analysis.

Analyses were performed by untargeted LC-MS/MS. Briefly, samples were separated over a reversed phase Phenomenex Kinetex C18 + column (2.1 × 100 mm, 1.7 μm particle size) maintained at 40°C. For the 20-minute LC gradient, the mobile phase consisted of the following: solvent A (1.5-mM ammonium fluoride) and solvent B (100% acetonitrile). The gradient was the following: 0 to 12.0 minutes 5% B, to 100% B, 12.0 to 15.0 minutes hold at 100% B, 15.0-15.1100% to 5% B, 15.1-20.0 minutes 5%B. The Q Exactive mass spectrometer was operated in polarity switching mode, using both positive and negative ion modes, scanning in full MS mode (2-μ scans) from 66.7 to 1000 m/z at 70-000 resolution with an automatic gain control (AGC) target of 3e6. Source ionization settings were 4.5/3.0-kV spray voltage, respectively, for positive and negative modes. Source gas parameters were 20 sheath gas, 10 auxiliary gas at 250°C, and 4 sweep gas. Calibration was performed prior to analysis using the Pierce Positive and Negative Ion Calibration Solutions (Thermo Fisher Scientific). Integrated peak areas were then extracted manually using Quan Browser (Thermo Fisher Xcalibur ver. 2.7). Statistical significance was determined using *t* test.

NAD(P)H fluorescence detection. OK cells cultured at 1X OS for 72 hours were incubated overnight in starvation medium (DMEM [Sigma; D5030] supplemented with 1-g/L glucose, 3.7-g/L sodium bicarbonate and 0.58-g/L glutamine). After washing twice with PBS, a rectangular section was excised from each filter, placed onto a MatTek dish, and covered with 50 μL of base medium (DMEM [Sigma; D5030] supplemented with 3.7-g/L sodium bicarbonate, and 3.6-g/L HEPES, pH 7.3] spiked with 2.24-g/L lactate or 3.15-g/L glucose, and overlaid with a coverglass. For live imaging, cells were maintained at 37°C and 5% CO_2 and imaged with a standard 4',6-diamidino-2-phenylindole filter set on a Leica DMi8 microscope equipped with a 40×/1.10 water objective and Leica DFC365 FX camera. For each treatment group, five stacks were acquired at 15-minute intervals with identical settings, 3 × 3 binning, and a step size of 2 μm. For image processing, Fiji was used to quantify each slice in each stack. Background was subtracted, and images were consistently thresholded to obtain integrated intensity through the stacks. Leica LAS X was used to generate 3D volume images. Based on the quantification, the two highest intensity slices from the stack were cropped from the original stack, the lowest 20% signal was removed considering as background, and pseudocolor scale was applied for easy interpretation.

Spatial distribution of albumin uptake, Na^+/K^+-ATPase, and Cox4. OK cells were cultured on 6-well (24-mm diameter) filter supports under static conditions (0X OS) or at 73 rpm (0.5X OS) for 72 hours, and then incubated for 15 minutes at 37°C with 500 μL apically added 50-μg/mL AlexaFluor-647 albumin in DMEM/F12 medium supplemented with 25-mM HEPES, pH 7.2-7.5. After washing in PBS, a ~24 × 10-mm strip running across the diameter of each filter was cut with a razor blade and divided into six roughly equivalent fractions (two each representing the edge, middle and center of the filter diameter). Each fraction was solubilized in lysis buffer, and the protein concentration was measured by Lowry assay. Albumin uptake was quantified by spectrofluorimetry and uptake in each fraction normalized for protein. Equal protein levels were run on SDS-PAGE gels and blotted to quantify Na^+/K^+-ATPase α subunit (Santa Cruz sc-21712; 1:200) and the mitochondrial marker Cox4 (Novus Biologicals NB110-39115; 1:1000). To quantify spatial differences in albumin uptake and protein distribution across the filter, the total signal in the six sections from each 0.5X OS filter was summed, and the percentage in each fraction relative to this total was calculated. Statistical significance was determined by *t* test.

ACKNOWLEDGMENTS

We thank Rob O'Doherty for helpful discussions and advice. We are grateful for the outstanding services provided by the University of Pittsburgh School of Medicine Genomics Analysis Core, the Biomedical Informatics Core, the Health Sciences Metabolomics and Lipidomics Core, the Center for Metabolism and Mitochondrial Medicine, and the Pittsburgh Center for Kidney Research (P30 DK079307). We are grateful for support from the University of Pittsburgh Center for Research Computing through the resources provided. This project was supported by National Institutes of Health (R01 DK101484, R01 DK100357, and 1S10OD021627) to O.A.W. M.J.J. was supported by National Institutes of Health (R01 DK114012 and R03 DK112044). Q.R. was supported by China Scholarship Council. M.L.G. was supported by National Institutes of Health (T32 DK061296 and TL1 TR001858). L.R.E. was supported by National Institutes of Health (T32 DK007052 and F32 DK117587).

ORCID

Ora A. Weisz https://orcid.org/0000-0003-2985-4870

REFERENCES

1. Hansell P, Welch WJ, Blantz RC, Palm F. Determinants of kidney oxygen consumption and their relationship to tissue oxygen tension in diabetes and hypertension. *Clin Exp Pharmacol Physiol*. 2013;40(2):123-137. https://doi.org/10.1111/1440-1681.12034.

2. Guder WG, Wagner S, Wirthensohn G. Metabolic fuels along the nephron: pathways and intracellular mechanisms of interaction. *Kidney Int*. 1986;29(1):41-45. https://doi.org/10.1038/ki.1986.6.
3. Forbes JM, Thorburn DR. Mitochondrial dysfunction in diabetic kidney disease. *Nat Rev Nephrol*. 2018;14(5):291-312. https://doi.org/10.1038/nrneph.2018.9.
4. Long KR, Shipman KE, Rbaibi Y, et al. Proximal tubule apical endocytosis is modulated by fluid shear stress via an mTOR-dependent pathway. *Mol Biol Cell*. 2017;28(19):2508-2517. https://doi.org/10.1091/mbc.E17-04-0211.
5. Krämer A, Green J, Pollard J, Tugendreich S. Causal analysis approaches in ingenuity pathway analysis. *Bioinformatics*. 2014;30(4):523-530. https://doi.org/10.1093/bioinformatics/btt703.
6. Sacktor B. Trehalase and the transport of glucose in the mammalian kidney and intestine. *Proc Natl Acad Sci USA*. 1968;60(3):1007-1014.
7. Bishop MJ, Everse J, Kaplan NO. Identification of lactate dehydrogenase isoenzymes by rapid kinetics. *Proc Natl Acad Sci USA*. 1972;69(7):1761-1765.
8. Lee JW, Chou C-L, Knepper MA. Deep sequencing in microdissected renal tubules identifies nephron segment-specific transcriptomes. *J Am Soc Nephrol*. 2015;26(11):2669-2677. https://doi.org/10.1681/ASN.2014111067.
9. Blacker TS, Duchen MR. Investigating mitochondrial redox state using NADH and NADPH autofluorescence. *Free Radic Biol Med*. 2016;100:53-65. https://doi.org/10.1016/j.freeradbiomed.2016.08.010.
10. Gstraunthaler G, Seppi T, Pfaller W. Impact of culture conditions, culture media volumes, and glucose content on metabolic properties of renal epithelial cell cultures. Are renal cells in tissue culture hypoxic? *Cell Physiol Biochem*. 1999;9(3):150-172.
11. Aleo MD, Schnellmann RG. Regulation of glycolytic metabolism during long-term primary culture of renal proximal tubule cells. *Am J Physiol*. 1992;262(1 pt 2):F77-F85. https://doi.org/10.1152/ajprenal.1992.262.1.F77.
12. Nowak G, Schnellmann RG. Improved culture conditions stimulate gluconeogenesis in primary cultures of renal proximal tubule cells. *Am J Physiol*. 1995;268(4 pt 1):C1053-C1061. https://doi.org/10.1152/ajpcell.1995.268.4.C1053.
13. Tang MJ, Suresh KR, Tannen RL. Carbohydrate metabolism by primary cultures of rabbit proximal tubules. *Am J Physiol*. 1989;256(3 pt 1):C532-C539. https://doi.org/10.1152/ajpcell.1989.256.3.C532.
14. Griner RD, Schnellmann RG. Decreasing glycolysis increases sensitivity to mitochondrial inhibition in primary cultures of renal proximal tubule cells. *In Vitro Cell Dev Biol Anim*. 1994;30A(1):30-34.
15. Monteil C, Leclere C, Dantzer F, Elkaz V, Fillastre JP, Morin JP. Modulation of glycolysis induction in primary cultures of rabbit kidney proximal tubule cells: the role of shaking, glucose and insulin. *Cell Biol Int*. 1993;17(10):953-960. https://doi.org/10.1006/cbir.1993.1019.
16. Sahai A, Cole LA, Clarke DL, Tannen RL. Rocking promotes differentiated properties in LLC-PK cells by improved oxygenation. *Am J Physiol*. 1989;256(5 pt 1):C1064-C1069. https://doi.org/10.1152/ajpcell.1989.256.5.C1064.
17. Cole LA, Scheid JM, Tannen RL. Induction of mitochondrial metabolism and pH-modulated ammoniagenesis by rocking LLC-PK1 cells. *Am J Physiol*. 1986;251(2 pt 1):C293-C298. https://doi.org/10.1152/ajpcell.1986.251.2.C293.
18. Dickman KG, Mandel LJ. Glycolytic and oxidative metabolism in primary renal proximal tubule cultures. *Am J Physiol*. 1989;257(2 pt 1):C333-C340. https://doi.org/10.1152/ajpcell.1989.257.2.C333.
19. Metzen E, Wolff M, Fandrey J, Jelkmann W. Pericellular PO2 and O2 consumption in monolayer cell cultures. *Respir Physiol*. 1995;100(2):101-106. https://doi.org/10.1016/0034-5687(94)00125-J.
20. Wolff M, Fandrey J, Jelkmann W. Microelectrode measurements of pericellular PO2 in erythropoietin-producing human hepatoma cell cultures. *Am J Physiol*. 1993;265(5 pt 1):C1266-C1270. https://doi.org/10.1152/ajpcell.1993.265.5.C1266.
21. Essig M, Friedlander G. Shear-stress-responsive signal transduction mechanisms in renal proximal tubule cells. *Curr Opin Nephrol Hypertens*. 2003;12(1):31-34. https://doi.org/10.1097/01.mnh.0000049808.98789.9a.
22. Mammoto A, Mammoto T, Ingber DE. Mechanosensitive mechanisms in transcriptional regulation. *J Cell Sci*. 2012;125:3061-3073. https://doi.org/10.1242/jcs.093005.
23. Agani F, Jiang B-H. Oxygen-independent regulation of HIF-1: novel involvement of PI3K/AKT/mTOR pathway in cancer. *Curr Cancer Drug Targets*. 2013;13(3):245-251. https://doi.org/10.2174/1568009611313030003.
24. Toschi A, Lee E, Gadir N, Ohh M, Foster DA. Differential dependence of hypoxia-inducible factors 1 alpha and 2 alpha on mTORC1 and mTORC2. *J Biol Chem*. 2008;283(50):34495-34499. https://doi.org/10.1074/jbc.C800170200.
25. Brugarolas J, Lei K, Hurley RL, et al. Regulation of mTOR function in response to hypoxia by REDD1 and the TSC1/TSC2 tumor suppressor complex. *Genes Dev*. 2004;18(23):2893-2904. https://doi.org/10.1101/gad.1256804.
26. Salek MM, Sattari P, Martinuzzi RJ. Analysis of fluid flow and wall shear stress patterns inside partially filled agitated culture well plates. *Ann Biomed Eng*. 2012;40(3):707-728. https://doi.org/10.1007/s10439-011-0444-9.
27. Thomas JMD, Chakraborty A, Sharp MK, Berson RE. Spatial and temporal resolution of shear in an orbiting petri dish. *Biotechnol Prog*. 2011;27(2):460-465. https://doi.org/10.1002/btpr.507.
28. Kim J-W, Dang CV. Multifaceted roles of glycolytic enzymes. *Trends Biochem Sci*. 2005;30(3):142-150. https://doi.org/10.1016/j.tibs.2005.01.005.
29. Lu Z, Hunter T. Metabolic kinases moonlighting as protein kinases. *Trends Biochem Sci*. 2018;43(4):301-310. https://doi.org/10.1016/j.tibs.2018.01.006.
30. Raghavan V, Rbaibi Y, Pastor-Soler NM, Carattino MD, Weisz OA. Shear stress-dependent regulation of apical endocytosis in renal proximal tubule cells mediated by primary cilia. *Proc Natl Acad Sci USA*. 2014;111(23):8506-8511. https://doi.org/10.1073/pnas.1402195111.
31. Raghavan V, Weisz OA. Discerning the role of mechanosensors in regulating proximal tubule function. *Am J Physiol Renal Physiol*. 2016;310(1):F1-F5. https://doi.org/10.1152/ajprenal.00373.2015.
32. Bhattacharyya S, Jean-Alphonse FG, Raghavan V, et al. Cdc42 activation couples fluid shear stress to apical endocytosis in proximal tubule cells. *Physiol Rep*. 2017;5(19):e13460. https://doi.org/10.14814/phy2.13460.
33. Weinbaum S, Duan Y, Satlin LM, Wang T, Weinstein AM. Mechanotransduction in the renal tubule. *Am J Physiol Renal Physiol*. 2010;299(6):F1220-F1236. https://doi.org/10.1152/ajprenal.00453.2010.
34. Wang T, Weinbaum S, Weinstein AM. Regulation of glomerulotubular balance: flow-activated proximal tubule function. *Pflugers Arch*. 2017;469(5–6):643-654. https://doi.org/10.1007/s00424-017-1960-8.
35. Du Z, Yan Q, Duan Y, Weinbaum S, Weinstein AM, Wang T. Axial flow modulates proximal tubule NHE3 and H-ATPase activities by changing microvillus bending moments. *Am J Physiol Renal Physiol*. 2006;290(2):F289-F296. https://doi.org/10.1152/ajprenal.00255.2005.
36. Duan Y, Weinstein AM, Weinbaum S, Wang T. Shear stress-induced changes of membrane transporter localization and expression in mouse proximal tubule cells. *Proc Natl Acad Sci USA*. 2010;107(50):21860-21865. https://doi.org/10.1073/pnas.1015751107.
37. Schnaper HW. The tubulointerstitial pathophysiology of progressive kidney disease. *Adv Chronic Kidney Dis*. 2017;24(2):107-116. https://doi.org/10.1053/j.ackd.2016.11.011.
38. Nourbakhsh N, Singh P. Role of renal oxygenation and mitochondrial function in the pathophysiology of acute kidney injury.

Nephron Clin Pract. 2014;127(1–4):149-152. https://doi.org/10.1159/000363545.
39. Shepard BD, Pluznick JL. Saving the sweetness: renal glucose handling in health and disease. *Am J Physiol Renal Physiol*. 2017;313(1):F55-F61. https://doi.org/10.1152/ajprenal.00046.2017.
40. Padovano V, Podrini C, Boletta A, Caplan MJ. Metabolism and mitochondria in polycystic kidney disease research and therapy. *Nat Rev Nephrol*. 2018;14(11):678-687. https://doi.org/10.1038/s41581-018-0051-1.
41. Padovano V, Kuo IY, Stavola LK, et al. The polycystins are modulated by cellular oxygen-sensing pathways and regulate mitochondrial function. *Mol Biol Cell*. 2017;28(2):261-269. https://doi.org/10.1091/mbc.E16-08-0597.
42. Gilbert RE. Proximal tubulopathy: prime mover and key therapeutic target in diabetic kidney disease. *Diabetes*. 2017;66(4):791-800. https://doi.org/10.2337/db16-0796.
43. Lieberthal W, Levine JS. Mammalian target of rapamycin and the kidney. I. The signaling pathway. *Am J Physiol Renal Physiol*. 2012;303(1):F1-F10. https://doi.org/10.1152/ajprenal.00014.2012.
44. Maxwell P. HIF-1: an oxygen response system with special relevance to the kidney. *J Am Soc Nephrol*. 2003;14(11):2712-2722. https://doi.org/10.1097/01.ASN.0000092792.97122.E0.
45. Orhon I, Dupont N, Codogno P. Primary cilium and autophagy: The avengers of cell-size regulation. *Autophagy*. 2016;12(11):2258-2259. https://doi.org/10.1080/15548627.2016.1212790.
46. Arici M, Brown J, Walls J, Bevington A. Free amino acids mimic the anabolic but not the proliferative effect of albumin in OK proximal tubular cells. *Cell Biochem Funct*. 2004;22(1):1-7. https://doi.org/10.1002/cbf.1045.
47. Grahammer F, Ramakrishnan SK, Rinschen MM, et al. mTOR regulates endocytosis and nutrient transport in proximal tubular cells. *J Am Soc Nephrol*. 2017;28(1):230-241. https://doi.org/10.1681/ASN.2015111224.
48. Eshbach ML, Sethi R, Avula R, et al. The transcriptome of the *Didelphis virginiana* opossum kidney OK proximal tubule cell line. *Am J Physiol Renal Physiol*. 2017;313(3):F585-F595. https://doi.org/10.1152/ajprenal.00228.2017.
49. Martin M. Cutadapt removes adapter sequences from high-throughput sequencing reads. *EMBnet J*. 2011;17(1):10. https://doi.org/10.14806/ej.17.1.200.
50. Kim D, Pertea G, Trapnell C, Pimentel H, Kelley R, Salzberg SL. TopHat2: accurate alignment of transcriptomes in the presence of insertions, deletions and gene fusions. *Genome Biol*. 2013;14(4):R36. https://doi.org/10.1186/gb-2013-14-4-r36.
51. Liao Y, Smyth GK, Shi W. featureCounts: an efficient general purpose program for assigning sequence reads to genomic features. *Bioinformatics*. 2014;30(7):923-930. https://doi.org/10.1093/bioinformatics/btt656.
52. Love MI, Huber W, Anders S. Moderated estimation of fold change and' ' dispersion for RNA-seq data with DESeq2. *Genome Biol*. 2014;15(12):550. https://doi.org/10.1186/s13059-014-0550-8.
53. Leek JT, Johnson WE, Parker HS, Jaffe AE, Storey JD. The sva package for removing batch effects and other unwanted variation in high-throughput experiments. *Bioinformatics*. 2012;28(6):882-883. https://doi.org/10.1093/bioinformatics/bts034.
54. Johnson WE, Li C, Rabinovic A. Adjusting batch effects in microarray expression data using empirical Bayes methods. *Biostatistics*. 2007;8(1):118-127. https://doi.org/10.1093/biostatistics/kxj037.
55. Sakai R, Winand R, Verbeiren T, Moere AV, Aerts J. dendsort: modular leaf ordering methods for dendrogram representations in R [version 1; peer review: 2 approved]. *F1000Res*. 2014;3:177. https://doi.org/10.12688/f1000research.4784.1.

SUPPORTING INFORMATION

Additional supporting information may be found online in the Supporting Information section at the end of this article.

How to cite this article: Ren Q, Gliozzi ML, Rittenhouse NL, et al. Shear stress and oxygen availability drive differential changes in opossum kidney proximal tubule cell metabolism and endocytosis. *Traffic*. 2019;1–12. https://doi.org/10.1111/tra.12648

Graphical Abstract

The contents of this page will be used as part of the graphical abstract on the HTML only. The graphical image and text will not be published as part of the final PDF copy.

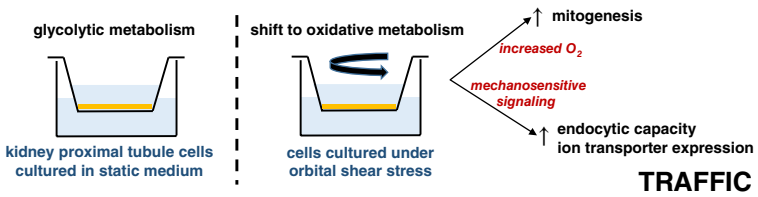

The proximal tubule (PT) relies primarily on oxidative metabolism rather than glycolysis to meet the high-energy demands needed to drive ion transport and endocytic reclamation of filtered proteins. Many of the available model cell lines fail to replicate the key features of this nephron segment. We found that culturing PT cells under continuous shear stress enhances cell differentiation and drives a metabolic shift toward oxidative metabolism. Moreover, oxygen availability and shear stress differentially regulate PT responses in this culture model.